

## Research Article

# An Adaptive WLAN Interference Mitigation Scheme for ZigBee Sensor Networks

Jo Woon Chong,<sup>1</sup> Chae Ho Cho,<sup>2</sup> Ho Young Hwang,<sup>3</sup> and Dan Keun Sung<sup>4</sup>

<sup>1</sup>Department of Biomedical Engineering, Worcester Polytechnic Institute, 100 Institute Road, Worcester, MA 01609, USA

<sup>2</sup>Department of Biomedical Engineering, University of Connecticut, Storrs, CT 06269, USA

<sup>3</sup>Department of Computer Engineering, Kwangwoon University, 20 Gwangun-ro, Nowon-gu, Seoul 139-701, Republic of Korea

<sup>4</sup>Department of Electrical Engineering, Korea Advanced Institute of Science and Technology, 291 Daehak-ro, Yuseong-gu, Daejeon 305-338, Republic of Korea

Correspondence should be addressed to Dan Keun Sung; [dksung@ee.kaist.ac.kr](mailto:dksung@ee.kaist.ac.kr)

Received 23 April 2015; Revised 19 June 2015; Accepted 27 July 2015

Academic Editor: Jaime Lloret

Copyright © 2015 Jo Woon Chong et al. This is an open access article distributed under the Creative Commons Attribution License, which permits unrestricted use, distribution, and reproduction in any medium, provided the original work is properly cited.

We propose an adaptive interference avoidance scheme that enhances the performance of ZigBee networks by adapting ZigBee's transmissions to measured wireless local area network (WLAN) interference. Our proposed algorithm is based on a stochastic analysis of ZigBee operation that is interfered with by WLAN transmission, given ZigBee and WLAN channels are overlaid in the industrial, scientific, and medical (ISM) band. We assume that WLAN devices have higher transmission power than ZigBee devices. Then, the high transmission power of WLAN devices causes the capture effect when WLAN and ZigBee transmit simultaneously. On the other hand, ZigBee performs backoff during clear channel assessment (CCA) operation if the WLAN is transmitting its frames on the channel. We adopt a widely used WLAN queueing/transmission model that is based on a Markov chain concept. We model a ZigBee device's operation using the Markov chain that includes WLAN interference statistically derived from the WLAN queueing/transmission model. Our proposed algorithm is evaluated in a simulated ZigBee network in the presence of varying WLAN interference. Numerical results show that our WLAN interference mitigation scheme finds the ZigBee control parameters, among a candidate set, which enhances ZigBee network performance compared to the conventional ZigBee operation.

## 1. Introduction

Wireless local area network (WLAN), Bluetooth, and ZigBee technologies have been adopted in various types of devices as user demands for wireless services in local or personal areas increase. For example, WLAN access points (APs) have been widely deployed in indoor or outdoor environments, and tablets or laptops use WLAN technology for an internet connection. Bluetooth technology has been used in wireless headsets for audio devices, hands-free sets for mobile phones, and wireless keyboards and mice for personal computers. ZigBee technology has gained attention from many companies since it consumes relatively less energy than other wireless technologies and can be implemented at low cost [1]. However, WLAN, Bluetooth, and ZigBee devices all operate on the 2.4 GHz industrial, scientific, and medical (ISM) band; hence if they coexist, they interfere with one another [2–6].

ZigBee's are required to conform to the physical layer (PHY) and medium access control (MAC) techniques of IEEE 802.15.4, which is standardized for low-rate wireless personal area networks (WPANs). IEEE 802.15.4 defines operations in the 2.4 GHz (worldwide), 868 MHz (Europe), and 915 MHz (Americas and Australia) ISM bands [7–10]. The maximum data rate is 250 kbps per channel and the transmission distance is around 10–20 m in indoor environment. The ZigBee protocol supports both beacon-enabled and beaconless modes. In the beacon-enabled mode [11], a coordinator synchronizes nodes by sending beacons. A superframe is limited by two consecutive beacons and is composed of active and inactive periods. The active period can be divided into a contention access period (CAP) and a contention-free period (CFP). Slotted carrier sense multiple access/collision avoidance (CSMA/CA) and time division multiple access (TDMA) are channel access modes in CAP

and CFP, respectively [12–16]. In the beaconless mode, unslotted CSMA/CA is a channel access mode. During the inactive period in a superframe, all the nodes go into sleep.

Slotted and unslotted CSMA/CA mechanisms perform operations of initialization, backoff, clear channel assessment (CCA), starting the transmission, and acknowledgement (optional) [17, 18]. Initialization is a procedure of setting a node's local backoff exponent variable to an initial value whenever a frame is successfully transmitted by the node. The backoff is a procedure of keeping the node silent before trying to assess the channel medium. This backoff lowers a frame collision probability by randomizing its channel assessment time. After the backoff, the node performs CCA. If the channel is assessed to be busy, the node performs backoff again after doubling backoff window size. This is to reduce a frame collision probability [19]. If the channel is assessed to be free during two CCAs, on the contrary, it starts its transmission. If the sending node requires an acknowledgement, the receiving node transmits an acknowledgement when the transmission is successful. Otherwise, the sending node regards it as transmission failure and retransmits its frame.

WLAN and Bluetooth devices have higher transmission powers compared to ZigBee devices by a factor of approximately ten to thousand times [17, 20]. In particular, the operating bandwidth of WLAN devices is wider than that of ZigBee devices; hence, if WLAN and ZigBee devices coexist and their operating bands are overlaid, the performance of ZigBee networks can be severely degraded by WLAN networks. On the other hand, WLAN transmission can be merely interfered with by ZigBee's transmissions. In this paper, we evaluate the performance of ZigBee networks interfered with by WLAN networks and propose an adaptive WLAN interference mitigation scheme for ZigBee networks. Our algorithm is based on the analysis and design of ZigBee's medium access control (MAC) operation when the ZigBee's are interfered with by WLAN transmissions. Our heterogeneous interference analysis is based on a Markov chain concept, adopting WLAN and ZigBee operation models from IEEE 802.11 and IEEE 802.15.4 specifications, respectively [20, 21]. The proposed interference avoidance algorithm adapts ZigBee's transmissions to the measured WLAN interference, in order to maximize ZigBee networks' performance. Our proposed unified analysis and design of ZigBee networks have wide applicability in that they can be utilized in predicting and enhancing the performance of random access MAC-based networks interfered with by other heterogeneous random access MAC-based networks or virtual slot-based networks.

The rest of this paper is organized as follows. We describe related work in Section 2. ZigBee and WLAN protocols are explained in Section 3. The coexisting ZigBee and WLAN network environment that we consider is presented. In Section 4, the ZigBee operation interfered with by WLAN transmissions is modeled based on a stochastic analysis with a Markov chain concept. Interference avoidance algorithms for ZigBee networks interfered with by WLAN are proposed in Section 5. Section 6 describes performance measures and

gives analytical and simulation results. Finally, Section 7 concludes this paper.

## 2. Related Work

The mutual interference problems among WLAN, Bluetooth, and ZigBee networks in the 2.4 GHz ISM band have been investigated in [22–30]. In [22, 23], the ZigBee frame error rate (FER) was measured when ZigBee devices coexist with WLANs and microwave ovens. Cochannel interference among ZigBee, Bluetooth, WLAN, and microwave ovens was evaluated in terms of frame loss of each system in [24]. The ZigBee packet error rate (PER) was evaluated through simulation when WLAN transmissions interfere with ZigBee's operation [25]. The opposite interference analysis, that is, ZigBee devices' interference on WLAN, was performed in [26, 27], which suggests that the effect of ZigBee transmissions on the WLAN is relatively insignificant compared to the reverse. In physical (PHY) layer, the performance of IEEE 802.15.4 ZigBee in the presence of IEEE WLAN (802.11b) and/or Bluetooth interference was analyzed in [28]. Here, they obtained the bit error rate (BER) performance under a varying signal-to-interference-plus noise ratio (SINR). In [29], the coexistence of ZigBee and WLAN in smart grid environments was investigated by measuring ZigBee's PER when ZigBee coexists with WLAN. In these studies, the interference is observed mainly in the PHY layer, and the WLAN interference to ZigBee is observed to be relatively severer than the reverse. This is due to the higher transmission power of WLAN devices compared to that of ZigBee devices. To standardize a coexistence algorithm for Bluetooth networks interfered with by WLAN networks, IEEE 802.15.2 working group (WG) has investigated the interference between WLAN and Bluetooth networks [30]. However, it focused on not ZigBee but Bluetooth.

The previous studies related to interference analysis mainly dealt with the operation among homogeneous ZigBee devices [31–33] or WLAN devices [34–38] without considering the heterogeneous interaction between ZigBee and WLAN. There exist analysis studies on the ZigBee's MAC operation interfered with by WLAN, but the WLAN interference is modeled by unrealistic the M/G/1 model [39, 40]. We model a WLAN queueing/transmission model reflecting a realistic WLAN MAC operation and transmission procedure, that is, CSMA/CA [34, 41]. The ZigBee network performance interfered with by WLAN interference is modeled by a Markov chain concept with WLAN interference parameterized in the Markov chain model. The proposed interference avoidance algorithm maximizes ZigBee networks' performance, for example, throughput, delay, and energy consumption, by controlling ZigBee's MAC parameters as well as ZigBee's frame size based on this analysis results.

The previous studies of the interference between WLAN and ZigBee [2–6] suggested that the way of mitigating the interference between WLAN and ZigBee is for ZigBee devices to avoid WLAN operating channels when ZigBee devices use their channels. Here, static and dynamic channel assignment methods are considered. The static assignment can be ineffective when the number of WLAN APs increases

or nodes are mobile [3] while the dynamic assignment methods can address these problems by avoiding nearby WLAN channels [42, 43]. However, these dynamic methods also become inefficient when there exists little WLAN traffic [2, 44]. The interference problems have also been investigated in the aspects of wireless sensor placement or sensor network topology [45–47]. In [45], the signal strength within an area is measured for IEEE 802.11a/b/g/n while a method for determining the optimal sensor placement based on [45] was proposed, which led to a reduction in the number of sensors to cover the area in [46]. A proactive method mediating the interference of WLAN and ZigBee devices is proposed in [48], and another in [49], with the concept of fairness additionally considered. A coexistence algorithm enabling ZigBee links to exploit WLAN white is proposed in [50]. An error detection and recovery method using partial packets are proposed to enhance link reliability in [51].

### 3. System Model

**3.1. ZigBee and WLAN Networks.** A ZigBee network can be configured in star or peer-to-peer topology. In the star topology, one ZigBee device, which is a full-function device (FFD), becomes a personal area network coordinator (PNC). Other ZigBee devices, which can be either reduced-function devices (RFDs) or FFDs, communicate with each other under the control of PNC. ZigBee devices start communication after associating themselves with PNC. The peer-to-peer topology is different from the star topology in the fact that devices can directly communicate with each other without PNC's relaying role. A ZigBee has 16 channels in the 2.4 GHz ISM band. The operation channels of ZigBee devices in the same network are configured by the same channel. For MAC protocol, ZigBee devices can use either CSMA/CA (mandatory) or TDMA (optional) [17]. When ZigBee devices gain channel access, they transmit data using a direct sequence spread spectrum (DSSS) physical layer technique.

A WLAN network consists of basic service sets (BSSs), where WLAN devices communicate with each other under the control of access points (AP). Both IEEE 802.11b and IEEE 802.11g PHYs have thirteen channels, respectively, each of which has 22 MHz bandwidth [52, 53]. The WLAN devices within the same BSS contend for channel access to transmit their frames. IEEE 802.11 incorporates CSMA/CA and TDMA services in the MAC protocol. IEEE 802.11b and IEEE 802.11g use DSSS and orthogonal frequency division multiplexing (OFDM), respectively, in transmitting data.

Figure 1 illustrates coexisting WLAN and ZigBee networks. For PHY layer techniques, IEEE 802.11b and IEEE 802.11g for WLAN and IEEE 802.15.4 for ZigBee operating in the 2.4 GHz ISM band are considered. Hence, if their operating bands are overlaid, the WLAN operation band is considered to completely or significantly overlay ZigBee operation band [17, 52–54]. For MAC layer techniques, mandatory slotted CSMA/CA mechanisms of WLAN and ZigBee are considered. We mainly focus on the operation of MAC protocols. Figures 2 and 3 illustrate the CSMA/CA mechanisms of ZigBee and WLAN devices, respectively. The unit slot lengths of ZigBee, IEEE 802.11b, and IEEE 802.11g are

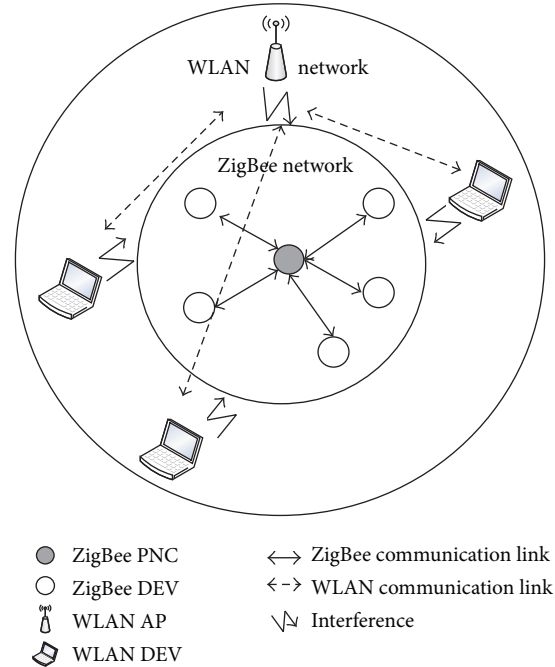


FIGURE 1: ZigBee and WLAN networks with mutual interference.

320  $\mu$ s, 20  $\mu$ s, and 9  $\mu$ s, respectively [17, 52, 53]. ZigBee and WLAN devices decrease their backoff counter values if the shared channel is not busy. However, ZigBee device senses its shared channel twice only after the backoff counter expires (when the backoff counter value reaches 0) while WLAN always senses its shared channel; hence, a ZigBee does not freeze its backoff counter during other ZigBee's transmissions unless its backoff counter expires while WLAN freezes it during other WLAN's transmissions. Also, ZigBee increases its backoff stage and randomly selects its backoff counter value when the channel is busy or its transmitted frame is collided while WLAN does the same procedure only when its transmitted frame is collided.

**3.2. Coexistence of ZigBee and WLAN: Medium Access Mechanisms.** Figure 4 shows three possible cases of simultaneous channel access from ZigBee and WLAN devices when they coexist, as shown in Figure 1. In *case 1*, when WLAN starts its transmission earlier, it ignores ZigBee transmission and keeps its transmission procedure. Here, the WLAN transmission includes both successful and collided WLAN transmissions. In *case 2*, on the other hand, when ZigBee starts its transmission earlier, it detects the WLAN transmission during CCA periods and defers its transmissions. In *case 3*, when WLAN and ZigBee start their transmissions at the same time, the WLAN transmission interferes with the ZigBee transmission while the ZigBee transmission does not. This is due to the difference between transmission powers of WLAN and ZigBee. Although there exists a skew between ZigBee and WLAN transmissions in *case 3*, the same analysis can be given since one ZigBee CCA duration (128  $\mu$ s) partially occupies the ZigBee unit slot (320  $\mu$ s). We statistically parametrize WLAN interference in Section 4 in the process of modeling the operation of ZigBee.

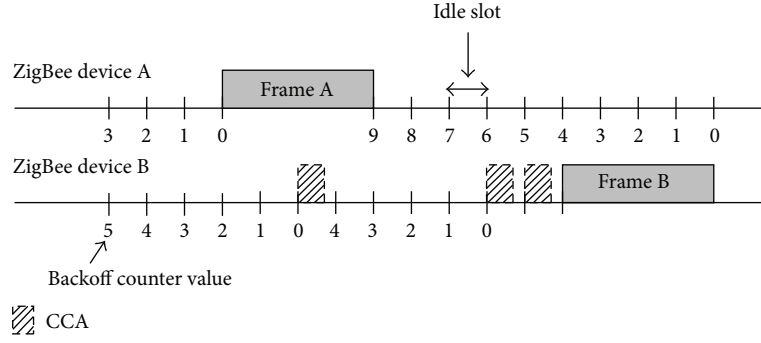


FIGURE 2: CSMA/CA mechanism of ZigBee devices.

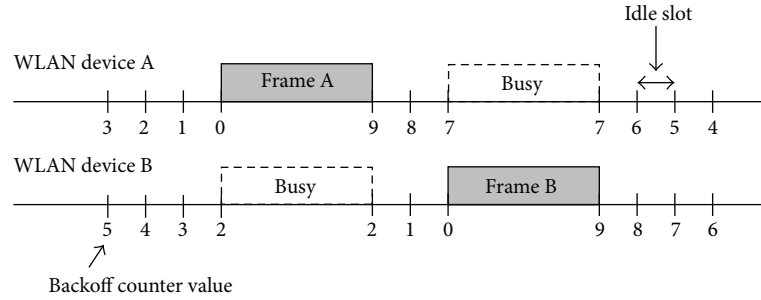


FIGURE 3: CSMA/CA mechanism of WLAN devices.

#### 4. ZigBee Operation Model Interfered with by WLAN Transmission

**4.1. ZigBee Operation: Markov Chain.** The operation of a ZigBee device is basically modeled by a Markov chain model as shown in Figure 5 [32]. A *node* in the Markov chain represents a *state*  $s_{i,j}$ , where  $i$  and  $j$  are backoff stage and backoff counter values, respectively. A *directed arrow* between two nodes indicates the direction of state transition, and the number on the directed arrow indicates the *transition probability* between states [55, 56]. The states can be classified into *backoff states* or *nonbackoff states* depending on the values  $i$  and  $j$ . The backoff state is defined as  $\{s_{i,j} \mid i \in [0, m], j \in [0, CW_i - 1]\}$ , where  $CW_i$  is the contention window size at backoff stage  $i$  and  $m$  is the maximum backoff stage value. The nonbackoff states are the remaining states, which cannot be reached by the backoff procedure but can be by the CCA procedure.

A ZigBee device initializes its operation at a randomly selected backoff state of the first row, that is,  $\{s_{i,j} \mid i = 0, j \in [0, CW_0 - 1]\}$ . The ZigBee decreases its backoff counter by one ( $j \rightarrow j - 1$ ) per each backoff unit slot  $\sigma$  until the counter reaches 0 ( $j = 0$ ). When  $j$  reaches 0, the ZigBee performs channel sensing, called CCA, to check channel occupancy. When the first CCA outcome informs that the channel is *busy*, the ZigBee increments its backoff stage by one ( $i \rightarrow i + 1$ ) and randomly selects  $j$  from  $[0, CW_{i+1} - 1]$ . If the channel is sensed as *idle*, the second CCA is performed. If the second CCA determines the channel is busy, the ZigBee does the same procedure as the busy case of the first CCA operation.

Otherwise, the device sends its frame to its corresponding receiver.

The transition probabilities between states are given by

$$\begin{aligned}
 \mathbb{P}\{s_{i,j} \mid s_{i,j+1}\} &= 1, \quad i \in (0, m), \quad j \in (0, CW_i - 2), \\
 \mathbb{P}\{s_{i,-1} \mid s_{i,0}\} &= 1 - \rho, \quad i \in (0, m), \\
 \mathbb{P}\{s_{i,j} \mid s_{i-1,0}\} &= \frac{\rho}{CW_i}, \\
 & \quad i \in (1, m), \quad j \in (0, CW_i - 1), \\
 \mathbb{P}\{s_{i,j} \mid s_{i-1,-1}\} &= \frac{\zeta}{CW_i}, \\
 & \quad i \in (1, m), \quad j \in (0, CW_i - 1), \quad (1) \\
 \mathbb{P}\{s_{0,j} \mid s_{i,-1}\} &= \frac{(1 - \zeta)}{CW_0}, \\
 & \quad i \in (1, m - 1), \quad j \in (0, CW_0 - 1), \\
 \mathbb{P}\{s_{0,j} \mid s_{m,0}\} &= \frac{\rho}{CW_0}, \quad j \in (0, CW_0 - 1), \\
 \mathbb{P}\{s_{0,j} \mid s_{m,-1}\} &= \frac{1}{CW_0}, \quad j \in (0, CW_0 - 1),
 \end{aligned}$$

where  $\rho$  and  $\zeta$  are the 1st and 2nd CCA busy probabilities, respectively. The WLAN interference is reflected in  $\rho$  and  $\zeta$  in this Markov chain. Since the parameters except  $\rho$  and

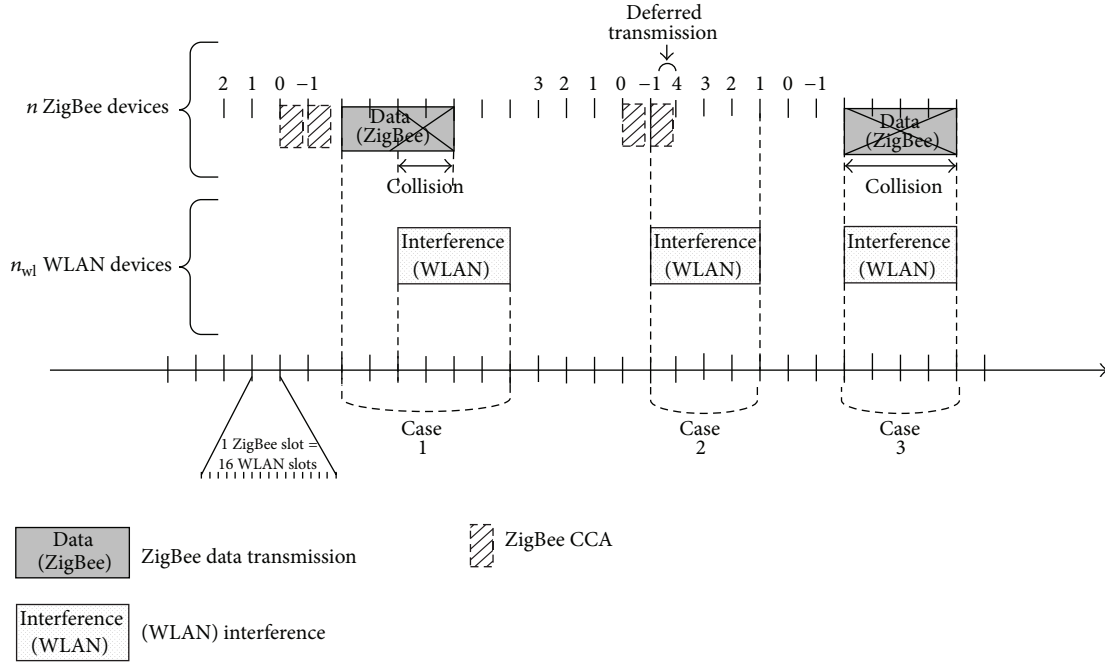


FIGURE 4: CCA operation of ZigBee devices interfered with by WLAN.

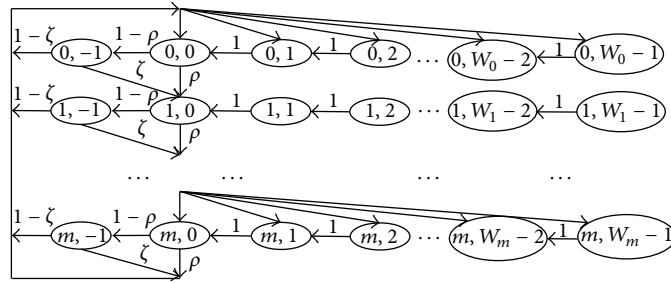


FIGURE 5: ZigBee operation model using a Markov chain concept.

$\zeta$  are given system parameters [17],  $\rho$  and  $\zeta$  need to be characterized to complete an analysis model for the ZigBee operation in the presence of WLAN interference.

To obtain  $\rho$  and  $\zeta$ , we tag one ZigBee which senses the shared channel even when  $j > 0$  but with turning off the connection between the CCA and backoff counter elements<sup>1</sup>. The tagged ZigBee operates the same in the CCA and transmission modes as other normal ZigBees. As a result,  $\rho$  and  $\zeta$  are equal to the first and second channel busy probabilities of this tagged ZigBee, respectively. Figure 6 shows an operation example of coexisting ZigBee and WLAN devices with a tagged ZigBee. The channel busy status is detected by the tagged ZigBee in three types of intervals: (i) only WLAN devices transmit frames (Intervals 1 and 7), (ii) only other ZigBee devices transmit frames (Intervals 2, 3, and 5), or (iii) WLAN and ZigBee devices simultaneously transmit frames (Interval 6). Hence,  $\rho$  is written by

$$\rho = \rho_{wl} + \rho_{zb} - \rho_{wl+zb}, \quad (2)$$

where  $\rho_{wl}$ ,  $\rho_{zb}$ , and  $\rho_{wl+zb}$  denote the tagged ZigBee's first channel busy probabilities caused by WLAN devices, other

ZigBee devices, and both of WLAN and ZigBee devices, respectively.

Similarly, the second CCA busy probability  $\zeta$  is written by

$$\zeta = \zeta_{wl} + \zeta_{zb} - \zeta_{wl+zb}, \quad (3)$$

where  $\zeta_{wl}$ ,  $\zeta_{zb}$ , and  $\zeta_{wl+zb}$  denote the tagged ZigBee's second channel busy probabilities caused by WLAN devices, other ZigBee devices, and both of WLAN and ZigBee devices, respectively.

**4.2. WLAN Interference Affecting ZigBee Clear Channel Assessment Operations:  $\rho$  and  $\zeta$ .** To derive  $\rho_{wl}$ , WLAN transmissions on the shared channel need to be analyzed in the viewpoint of the tagged ZigBee. Let  $\Psi_{wl}$ ,  $\sigma_{wl}$ , and  $T_{cca}$  be the number of WLAN consecutive idle slots, one WLAN backoff unit duration in seconds, and one ZigBee CCA duration in seconds, respectively. Specifically,  $\Psi_{wl}$  is a random variable, which can be counted in a network viewpoint, determined by WLAN transmission characteristics including transmission probability, success probability, collision probability, frame

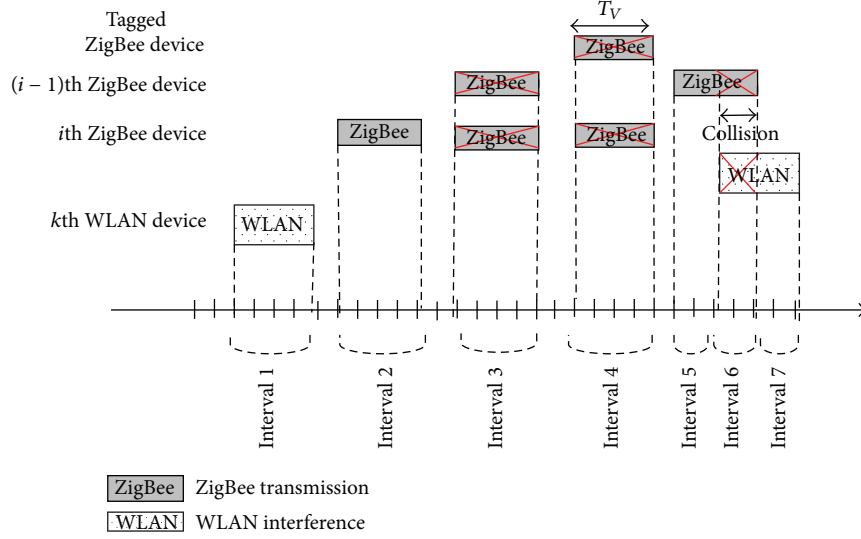


FIGURE 6: ZigBee transmission cases interfered with by WLAN.

length, and backoff unit duration. Then, two possible channel busy cases due to WLAN transmission can occur: (1) one ZigBee CCA duration is shorter than WLAN consecutive idle duration ( $T_{cca} < \Psi_{wl}\sigma_{wl}$ ) and (2) one ZigBee CCA duration is longer than WLAN consecutive idle duration ( $T_{cca} > \Psi_{wl}\sigma_{wl}$ ). If  $T_{cca} < \Psi_{wl}\sigma_{wl}$ , then  $\rho_{wl}$  is equal to WLAN channel activity. On the other hand, if  $T_{cca} > \Psi_{wl}\sigma_{wl}$ , then  $\rho_{wl}$  is equal to 1. Hence,  $\rho_{wl}$  is given by

$$\rho_{wl} = \mathbb{P}\{T_{cca} < \Psi_{wl}\sigma_{wl}\} \cdot \left[ \frac{p_{s_{wl}}(T_{s_{wl}} + T_{cca}) + (1 - p_{s_{wl}})(T_{c_{wl}} + T_{cca})}{\mathbb{E}\{\Psi_{wl}\}\sigma_{wl} + p_{s_{wl}}T_{s_{wl}} + (1 - p_{s_{wl}})T_{c_{wl}}} \right] + \mathbb{P}\{T_{cca} \geq \Psi_{wl}\sigma_{wl}\}, \quad (4)$$

where WLAN channel activity expressed in the first term is a function of successful transmission probability  $p_{s_{wl}}$ , successful transmission duration  $T_{s_{wl}}$ , and collision duration  $T_{c_{wl}}$  as well as  $\sigma_{wl}$ ,  $T_{cca}$ , and  $\mathbb{E}\{\Psi_{wl}\}$ . Note that  $\mathbb{E}\{\Psi_{wl}\}$  is a function of WLAN transmission probability  $\kappa_{wl}$  and the number of active WLAN devices  $n_{wl}$  as follows:

$$\mathbb{E}\{\Psi_{wl}\} = \frac{1}{1 - (1 - \kappa_{wl})^{n_{wl}}} - 1. \quad (5)$$

We can also approximate  $\mathbb{P}\{T_{cca} < \Psi_{wl}\sigma_{wl}\}$  as (see Appendix A)

$$\mathbb{P}\{T_{cca} < \Psi_{wl}\sigma_{wl}\} = (1 - \kappa_{wl})^{n_{wl}\lceil T_{cca}/\sigma_{wl} \rceil}, \quad (6)$$

where  $\lceil x \rceil$  denotes the ceiling function of  $x$ .

Using (4)–(6), we have

$$\rho_{wl} = \frac{(1 - \kappa_{wl})^{n_{wl}\lceil T_{cca}/\sigma_{wl} \rceil} [p_{s_{wl}}T_{s_{wl}} + (1 - p_{s_{wl}})T_{c_{wl}}]}{[1 / (1 - (1 - \kappa_{wl})^{n_{wl}}) - 1]\sigma_{wl} + p_{s_{wl}}T_{s_{wl}} + (1 - p_{s_{wl}})T_{c_{wl}}} + 1 - (1 - \kappa_{wl})^{n_{wl}\lceil T_{cca}/\sigma_{wl} \rceil}. \quad (7)$$

To derive  $\rho_{zb}$ , the ZigBee transmissions in terms of the tagged ZigBee need to be investigated. We first define the CCA-start probability  $\kappa$  of a ZigBee in backoff states as

$$\kappa = \frac{\sum_{i=0}^m \pi_{i,0}}{\sum_{i=0}^m \sum_{j=0}^{W_i-1} \pi_{i,j}} = \frac{2[1 - (\rho + \zeta - \rho\zeta)^{m+1}]}{\sum_{i=0}^m (CW_0 2^{\eta_i} + 1)(\rho + \zeta - \rho\zeta)^i} \times \frac{1}{1 - (\rho + \zeta - \rho\zeta)}, \quad (8)$$

where  $\pi_{i,j}$  is the stationary probability of  $s_{i,j}$  and  $\eta_i$  is the additional backoff exponent value of backoff stage  $i$ <sup>2</sup>. The denominator is a summation over backoff states ( $\{s_{i,j} \mid i \in [0, m], j \in [0, CW_i - 1]\}$ ) since CCA-start probability assumes that a device is in the backoff states.  $\eta_{max}$  and  $\eta_{min}$  are the maximum and minimum backoff exponent values, respectively. Then, we have  $\eta_i = \min\{i, \eta_{max} - \eta_{min}\}$ . Due to  $n - 1$  other ZigBee transmissions, two possible channel busy events of the tagged ZigBee can occur: successful and collided transmissions of other ZigBees. In the successful transmission interval, only one of other ZigBees reaches the CCA-start state with probability  $(n - 1)\kappa(1 - \kappa)^{n-1}$ , and WLAN devices do not interfere for two consecutive CCAs

with probability  $(1 - \rho_{wl})(1 - \zeta_{wl})$  and do not transmit during total ZigBee communication time with probability  $(1 - \kappa_{wl})^{\lceil L_{tx}(\sigma/\sigma_{wl}) \rceil n_{wl}}$ , where  $L_{tx}(\sigma/\sigma_{wl})$  denotes total ZigBee communication time. In the collided transmission, at least two other ZigBee devices reach the CCA-start state

$$\begin{aligned} p_t &= (1 - \kappa) \left[ 1 - (1 - \kappa)^{n-1} \right] (1 - \rho_{wl}) (1 - \zeta_{wl}), \\ p_s &= \frac{(n-1) \kappa (1 - \kappa)^{n-1} (1 - \rho_{wl}) (1 - \zeta_{wl}) (1 - \kappa_{wl})^{\lceil [L_f] + [\delta] + [L_{ack}] \rceil (\sigma/\sigma_{wl}) n_{wl}}}{p_t}, \end{aligned} \quad (9)$$

where  $L_f$  is the ZigBee frame length,  $\delta$  is the acknowledgement waiting time, and  $L_{ack}$  is the acknowledgement frame length.  $\lfloor x \rfloor$  denotes the floor function of  $x$ .

Consider that  $T_1, T_2, \dots$  is a sequence of intervals of successful transmissions of the tagged ZigBee, and  $W_1, W_2, \dots$  is a sequence of channel busy duration in  $T_1, T_2, \dots$ , respectively.  $T_1, T_2, \dots$  is a sequence of positive independent and identically distributed random variables such that

$$0 < \mathbb{E} \{T_{ij}\} < \infty \quad (10)$$

and  $W_1, W_2, \dots$  is a sequence of random variables (rewards) satisfying

$$\mathbb{E} \{W_i\} < \infty. \quad (11)$$

Let  $Y_t = \sum_{i=1}^{K_t} W_i$  where  $K_t = \sup\{n : J_n \leq t\}$  and  $J_n = \sum_{i=1}^n T_i$ . Using the elementary renewal theorem for renewal reward processes, we have

$$\lim_{t \rightarrow \infty} \frac{1}{t} \mathbb{E} \{Y_t\} = \frac{\mathbb{E} \{W_1\}}{\mathbb{E} \{T_1\}}. \quad (12)$$

Using (12),  $\rho_{zb}$  is given by

$$\rho_{zb} = \frac{p_t [p_s L_{bs} + (1 - p_s) L_{bc}]}{p_t [p_s L_s + (1 - p_s) L_c] + (1 - p_t)}, \quad (13)$$

where  $L_s$  and  $L_c$  are successful transmission and collision duration in ZigBee unit slots, respectively, and  $L_{bs}$  and  $L_{bc}$  are busy duration out of  $L_s$  and  $L_c$ , respectively.

$\rho_{wl+zb}$  is approximated as

$$\begin{aligned} \rho_{wl+zb} &\approx \rho_{zb} \left[ 1 - \frac{U_{wl} (1 - U_{wl}^{\lceil L_f \rceil + [\delta] + [L_{ack}]})}{1 - U_{wl}} \right. \\ &\quad \left. \cdot \frac{1}{\lceil L_f \rceil + [\delta] + [L_{ack}]} \right], \end{aligned} \quad (14)$$

where  $U_{wl} = (1 - \kappa_{wl})^{(\sigma/\sigma_{wl}) n_{wl}}$  is the probability that  $n_{wl}$  WLAN devices do not transmit data during  $\sigma$  (see Appendix B). Substituting (7), (13), and (18) into (2), we finally get  $\rho$ .

simultaneously with probability  $(1 - \kappa)[1 - (1 - \kappa)^{n-1} - (n-1)\kappa(1 - \kappa)^{n-2}]$ , and WLAN devices do not interfere for two consecutive CCAs  $(1 - \kappa_{wl})^{\lceil L_{tx}(\sigma/\sigma_{wl}) \rceil n_{wl}}$ . Let  $p_t$  and  $p_s$  be transmission and successful transmission probabilities of ZigBees except the tagged ZigBee, respectively. Then, we have

For the second CCA, two possible busy events can occur: (i)  $\Psi_{wl} \sigma_{wl} > \sigma + T_{cca}$ , that is, WLAN has longer consecutive idle duration compared to a unit backoff slot plus one CCA duration of a ZigBee, and (ii)  $T_{cca} \leq \Psi_{wl} \sigma_{wl} \leq \sigma + T_{cca}$ , that is, WLAN consecutive idle duration is in the range from one ZigBee CCA duration to a ZigBee backoff unit slot plus one ZigBee CCA duration. Hence, we have

$$\begin{aligned} \zeta_{wl} &\approx \mathbb{P} \{ \Psi_{wl} \sigma_{wl} > \lceil T_{cca} \rceil + T_{cca} \} \left( \frac{1}{1 - \rho_{wl}} \right) \\ &\quad \cdot \frac{\lceil T_{cca} \rceil}{\mathbb{E} \{ \Psi_{wl} \} \sigma_{wl} + p_{s_{wl}} T_{s_{wl}} + (1 - p_{s_{wl}}) T_{c_{wl}}} \\ &\quad + \sum_{x=\lceil T_{cca} \rceil / \sigma_{wl}}^{\lceil T_{cca} \rceil + T_{cca} / \sigma_{wl}} \mathbb{P} \{ \Psi_{wl} = x \} \left( \frac{1}{1 - \rho_{wl}} \right) \\ &\quad \cdot \frac{(x \sigma_{wl} - T_{cca})}{\mathbb{E} \{ \Psi_{wl} \} \sigma_{wl} + p_{s_{wl}} T_{s_{wl}} + (1 - p_{s_{wl}}) T_{c_{wl}}}. \end{aligned} \quad (15)$$

Using the approximations of  $\mathbb{P} \{ \Psi_{wl} \sigma_{wl} > \lceil T_{cca} \rceil + T_{cca} \}$  and  $\mathbb{P} \{ \Psi_{wl} = x \}$  in Appendix A, we get  $\zeta_{wl}$

$$\begin{aligned} \zeta_{wl} &\approx \left( \frac{1}{1 - \rho_{wl}} \right) \frac{(1 - \kappa_{wl})^{n_{wl}(\lceil T_{cca} \rceil + T_{cca}) / \sigma_{wl}} \lceil T_{cca} \rceil}{\mathbb{E} \{ \Psi_{wl} \} \sigma_{wl} + p_{s_{wl}} T_{s_{wl}} + (1 - p_{s_{wl}}) T_{c_{wl}}} + \left( \frac{1}{1 - \rho_{wl}} \right) \\ &\quad \cdot \frac{\sum_{x=\lceil T_{cca} \rceil / \sigma_{wl}}^{\lceil T_{cca} \rceil + T_{cca} / \sigma_{wl}} (1 - \kappa_{wl})^{n_{wl}(x-1)} [1 - (1 - \kappa_{wl})^{n_{wl}}] (x \sigma_{wl} - T_{cca})}{\mathbb{E} \{ \Psi_{wl} \} \sigma_{wl} + p_{s_{wl}} T_{s_{wl}} + (1 - p_{s_{wl}}) T_{c_{wl}}}. \end{aligned} \quad (16)$$

In addition,

$$\begin{aligned} \zeta_{zb} &= \left( \frac{1}{1 - \rho_{zb}} \right) \\ &\quad \cdot \frac{p_t [p_s L_{is} + (1 - p_s) L_{ic}]}{p_t [p_s L_s + (1 - p_s) L_c] + \kappa + (1 - \kappa - p_t)}, \end{aligned} \quad (17)$$

where  $L_{is}$  and  $L_{ic}$  denote the duration during which the second busy CCA events occur out of  $L_s$  and  $L_c$ , respectively. The second CCA is considered to be busy during the first slot of data or the acknowledgement transmission in the successful transmission case ( $p_s$ ) while it is considered to be busy, in the collision case ( $1 - p_s$ ), during the first slot of data transmission. Hence,  $L_{is} = 2\lceil L_{cca} \rceil$  and  $L_{ic} = \lceil L_{cca} \rceil$ .

Again, we have

$$\zeta_{wl+zb} \approx \zeta_{zb} \left[ 1 - p_s \frac{U_{wl} (1 - U_{wl}^{L_{is}})}{(1 - U_{wl})} \frac{1}{L_{is}} - (1 - p_s) \frac{U_{wl} (1 - U_{wl}^{L_{ic}})}{(1 - U_{wl})} \frac{1}{L_{ic}} \right], \quad (18)$$

where the second and third terms represent the ratios of simultaneous transmissions among ZigBee transmissions making the second CCA busy in the successful and collided transmission cases, respectively (see Appendix B). Substituting (16), (17), and (18) into (3), we finally get  $\zeta$ .

## 5. Adaptive Interference Avoidance Algorithm

Our proposed algorithm adaptively controls ZigBee transmissions based on the amount of WLAN interference to maximize the performance of ZigBee network. Our proposed method basically assumes that WLAN devices highly contend for channel access. First, a WLAN AP estimates the WLAN channel activity  $\rho_{wl}$ . The WLAN channel activity  $\rho_{wl}$  is monitored by a WLAN AP. For the number of associated WLAN nodes, a WLAN AP can keep track of it. However, some associated WLAN nodes may be inactive while the others are active. Here, it is difficult for a WLAN AP to directly know about the number  $N_{wl}$  of active WLAN nodes. The channel activity is reflected in  $\sum_{i=0}^{c-1} A[m]_i$  and  $\sum_{i=0}^{c-1} B[m]_i$  in (21) and (22), which are used to calculate  $N_{wl}$  in (20). WLAN AP then informs ZigBee of  $N_{wl}$  and  $\rho_{wl}$  from which the PNC calculates the number  $N_{zb}^*$  of ZigBee devices as well as the length  $L_{zb}^*$  for each ZigBee frame. The PNC broadcasts  $N_{zb}^*$  and  $L_{zb}^*$  to ZigBee devices which decide if they send data or not considering  $N_{zb}^*$  and the total number of Zigbee devices. This situation can be feasibly given when there are devices having both WLAN and ZigBee modules in a network. If a ZigBee device transmits, it sends its frame after segmenting the frame into the length of  $L_{zb}^*$ . This procedure repeats periodically.

*5.1. Autoregressive-Moving-Average (ARMA) Estimation of  $N_{wl}$ .*  $N_{wl}$  is estimated using the following expression [34]:

$$N_{wl} = \frac{\log(1 - p_{wl})}{\log(1 - \kappa_{wl})} + 1, \quad (19)$$

where  $\kappa_{wl}$  and  $p_{wl}$  are WLAN transmission and collision probabilities, respectively. The estimation of  $\kappa_{wl}$  and  $p_{wl}$  is derived by ARMA( $\beta, c$ ) [57]. First,  $\kappa_{wl}$  is estimated as follows:

$$\hat{\kappa}_{wl}[m+1] = \beta \hat{\kappa}_{wl}[m] + \frac{(1-\beta)}{c} \sum_{i=0}^{c-1} A[m]_i, \quad (20)$$

where  $c$  and  $\beta$  are the number of measured samples and ARMA model parameter, respectively.  $\kappa_{wl}[m]$  is transmission probability in the  $m$ th beacon interval.  $A[m]_i$  is 1 only if AP observes the beginning of the WLAN station's transmission

at the  $i$ th slot of the  $m$ th beacon interval. Otherwise,  $A[m]_i$  is 0.

Collision probability  $p_{wl}$  is similarly estimated as follows:

$$\hat{p}_{wl}[m+1] = \beta \hat{p}_{wl}[m] + \frac{(1-\beta)}{c} \sum_{i=0}^{c-1} B[m]_i, \quad (21)$$

where  $p_{wl}[m]$  is collision probability in the  $m$ th beacon interval and  $B[m]_i$  is 0 when the WLAN station observes the channel is idle or successfully transmits its frame at the  $i$ th slot of the  $m$ th beacon interval. On the other hand,  $B[m]_i$  is 1 when the WLAN station observes the channel is busy or transmits with collisions. We estimate  $p_{wl}$  and  $\kappa_{wl}$  periodically and recursively at the end of every beacon interval. When  $p_{wl}$  is equal to 0,  $N_{wl}$  is estimated to be 1.

*5.2. Determination of  $N_{zb}^*$  and  $L_{zb}^*$ .* ZigBee determines  $N_{zb}^*$  and  $L_{zb}^*$  which maximize ZigBee performance measures such as throughput, energy consumption, or delay.

The normalized throughput  $S$  is defined as

$$S = \frac{\text{successfully transmitted bits in a ZigBee network}}{\text{observation time (secs)}} \times \frac{1}{R}, \quad (22)$$

where  $R$  denotes ZigBee PHY data rate. Regarding the average time of state transition as a renewal period,  $\mathbb{E}\{S\}$  can be expressed as [32]

$$\mathbb{E}\{S\} = \frac{m\kappa(1-\kappa)^{n-1}(1-\rho)(1-\zeta)\gamma L_p}{(1-\kappa) + \kappa\rho + 2\kappa(1-\rho)\zeta + \kappa(1-\rho)(1-\zeta)\{\gamma L_s + (1-\gamma)L_c\}}, \quad (23)$$

where  $L_p$  is payload length in slots and  $\gamma$  is successful frame transmission probability after two successful CCAs. Since ZigBee sense a shared channel for only two successful CCAs, the frame successful transmission after CCAs is only dependent on WLAN transmissions. Hence, considering that  $\lceil \lceil L_{tx} \rceil (\sigma / \sigma_{wl}) \rceil$  is the number of WLAN slots within  $L_{tx}$ ,  $\gamma$  is expressed as

$$\gamma = (1 - \kappa_{wl})^{\lceil \lceil L_{tx} \rceil (\sigma / \sigma_{wl}) \rceil N_{wl}}, \quad (24)$$

where  $L_{tx}$  and  $\sigma_{wl}$  are transmission length in slots and WLAN's unit time, respectively.

The energy consumption  $E$  is defined as the amount of energy consumed per transmission unit slot by a ZigBee



network.  $\mathbb{E}\{E\}$  is expressed as [32]

$$\mathbb{E}\{E\} = \frac{\kappa\rho T_{cca}E_{rx} + \kappa(1-\rho)\zeta T_{cca}E_{rx} + \kappa(1-\rho)(1-\zeta)\{\gamma E_s + (1-\gamma)E_c\}}{\kappa(1-\rho)(1-\zeta)\gamma L_p}, \quad (25)$$

where  $E_{rx}$ ,  $E_s$ , and  $E_c$  are consumed energies for reception, successful transmission, and collision, respectively.

Access delay  $D$  is defined as elapsed interval from the time when the frame reaches the head-of-line of a transmitter's buffer and the time when the frame arrives at a receiver without collision. By Little's law [35],  $\mathbb{E}\{D\}$  is given as

$$\mathbb{E}\{D\} = \frac{n}{\mathbb{E}\{S\}/L_p} \cdot \sigma, \quad (26)$$

where  $\mathbb{E}\{S\}/L_p$  represents ZigBee frame delivery rate. Throughput, energy consumption, and delay are affected by WLAN parameters, for example,  $N_{wl}$  and  $\rho_{wl}$  (or  $\kappa_{wl}$ ) as shown in (23), (25), and (26). After receiving  $\widehat{N}_{wl}$  and  $\widehat{\kappa}_{wl}$  from a WLAN AP, the ZigBee PNC finds  $N_{zb}^*$  and  $L_{zb}^*$  that maximize required performance index, for example, throughput, energy consumption, or delay, depending on service requirements. For example, if  $\widehat{N}_{wl}$  and  $\widehat{\kappa}_{wl}$  are 3 and 0.12 with a constraint that energy consumption should be minimized, then the ZigBee PNC finds  $N_{zb}^*$  and  $L_{zb}^*$  minimizing (25). And it can be a problem if the energy consumption in calculating the number of interference nodes,  $N_{zb}^*$  and  $L_{zb}^*$ , surpasses the transmission energy saved by our proposed algorithm. However, the relatively stable nature of WLAN condition enables us to assume that the calculation does not occur too frequently. To reduce the computational complexity of the algorithm, we made a matching table in advance, which has inputs of  $N_{wl}$  and  $\rho_{wl}$  and gives outputs of  $N_{zb}^*$  and  $L_{zb}^*$  from the table.

## 6. Numerical Result

We configured coexisting ZigBee and WLAN networks using OPNET Modeler 14.5 as shown in Figure 7 and Matlab. A ZigBee network interfered with by saturated and unsaturated WLAN nodes is considered. Here, all the ZigBee devices in a network are considered to be affected by WLAN interference.

In our interference analysis, ZigBee devices are assumed to always have frames to transmit while IEEE 802.11b/g WLAN devices are considered to have frames that arrive at their buffers in a Poisson manner with the intensity of  $\lambda_{wl}$ . Hence, when we define  $q_{wl}$  as the probability of WLAN traffic generation in each slot,  $q_{wl} = \text{Exp}(-\lambda_{wl}T)$ . This analysis can be regarded as saturation mode analysis by increasing  $\lambda_{wl}$  and  $q_{wl}$ .  $\kappa_{wl}$  is expressed as in [41]:

$$\kappa_{wl} = \pi_{0,0}^{e_{wl}} \left( \frac{q_{wl}^2 W_{0,wl}}{(1-p_{wl})(1-q_{wl})(1-(1-q_{wl})^{W_{0,wl}})} - \frac{q_{wl}^2(1-p_{wl})}{1-q_{wl}} \right), \quad (27)$$

where  $\pi_{0,0}^{e_{wl}}$  is stationary probability of a device which has a backoff counter value of zero with no waiting frame.  $p_{wl}$  is the collision probability of a device. The expected slot time  $\mathbb{E}\{T\}$  can be derived as

$$\mathbb{E}\{T\} = (1-p_{tr,wl})\sigma_{wl} + p_{tr,wl}p_{s,wl}T_{s,wl} + p_{tr,wl}p_{c,wl}T_{c,wl}, \quad (28)$$

where  $p_{tr,wl}$ ,  $p_{s,wl}$ , and  $p_{c,wl}$  are transmission, success, and collision probabilities in a WLAN network, respectively, and  $p_{tr,wl} = 1 - (1 - \kappa_{wl})^{n_{wl}}$ ,  $p_{s,wl} = n_{wl}\kappa_{wl}(1 - \kappa_{wl})^{n_{wl}-1}$ , and  $p_{c,wl} = 1 - (1 - \kappa_{wl})^{n_{wl}} - n_{wl}\kappa_{wl}(1 - \kappa_{wl})^{n_{wl}-1}$ . Table 1 shows our WLAN and ZigBee parameter settings [17, 20, 21].  $L_s = 2[L_{cca}] + L_f + [\delta] + [L_{ack}]$ ,  $L_c = 2[L_{cca}] + L_f$ , and  $L_{bs} = L_{bc} = L_f$ .  $E_s$  and  $E_c$  are set to  $L_f E_{tx} + ([\delta] + T_{ack})E_{rx}$  and  $L_f E_{tx} + ([\delta] + T_{ack})E_{rx}$ , respectively.

Our analysis framework is verified by comparing throughput, delay, and energy consumption obtained from our framework with those from simulation results. Each simulation point is obtained by averaging over fifteen simulation run results with the duration of 600 seconds. The range bars are also drawn on the plot. Figure 8 shows a ZigBee network's normalized throughput  $\mathbb{E}\{S\}$  with varying WLAN interference load  $\lambda_{wl}$  when  $n$  and  $n_{wl}$  are fixed to 25 and 3. The analytical results obtained from the proposed model are validated and agree well with the simulation results. When the length of a ZigBee frame  $L_f$  is equal to 8 and  $\lambda_{wl}$  is set to 0.047,  $\mathbb{E}\{S\}$  is equal to 0.09. However, if the ZigBee network is interfered with by the WLAN with  $\lambda_{wl} = 0.116$ ,  $\mathbb{E}\{S\}$  decreases to 0.03. Fixing  $\lambda_{wl}$  to 0.047,  $\mathbb{E}\{S\}$  increases as  $L_{f,slot}$  gets larger because WLAN interference is not severe. However, when  $\lambda_{wl} = 0.139$ , as  $L_f$  increases from 8 to 12,  $\mathbb{E}\{S\}$  does not significantly change since the ZigBee frame is exposed to severe WLAN interference which causes more collisions between ZigBee and WLAN transmissions. Here,  $\mathbb{E}\{S\}$  exhibits a steeper decrease as  $L_f$  gets larger. Figures 10 and 12 show mean energy consumption  $\mathbb{E}\{E\}$  and access delay  $\mathbb{E}\{D\}$  for varying  $\lambda_{wl}$ . Similar to  $\mathbb{E}\{S\}$ , as  $L_f$  gets larger,  $\mathbb{E}\{E\}$  and  $\mathbb{E}\{D\}$  abruptly get worse. Figures 9, 11, and 13 show  $\mathbb{E}\{S\}$ ,  $\mathbb{E}\{E\}$ , and  $\mathbb{E}\{D\}$  of a ZigBee network when  $n_{wl}$  increases from 3 to 6 with the fixed total amount of WLAN network load,  $\lambda_{wl}$ . The ZigBee performance is slightly degraded when  $n_{wl}$  increases from 3 to 6 since more WLAN devices generate less ZigBee's transmission opportunities due to WLAN devices' increased contention on the shared channel. However, this degradation is not considerable since the total traffic load  $\lambda_{wl}$  is fixed and shared by WLAN devices.

For the saturated WLAN mode, the estimation of  $N_{wl}$  is done by simply measuring  $\kappa_{wl}$  and  $p_{wl}$ . Figure 7 shows a ZigBee network interfered with by WLAN interferers, where six Zigbee devices always have frames to transmit to a coordinator while WLAN transmissions are simply modeled

TABLE 1: WLAN and ZigBee related parameter values.

Parameter	Value	Description
$E_{rx}$	0.0113472 mJ	Energy consumption for ZigBee to receive (mJ)
$E_{tx}$	0.0100224 mJ	Energy consumption for ZigBee to transmit (mJ)
$L_{ack}$	1.1 slots	Length of Ack frame in ZigBee
$L_{cca}$	0.4 slots	One ZigBee CCA duration
$L_f$	4~20 slots	Length of a frame in ZigBee
$L_{nack}$	1.1 slots	Length of Nack duration in ZigBee
$L_p$	$L_f \times 80 - 120$ bits	Length of payload in ZigBee (bits)
$T_{collwl}$	944 $\mu$ s	Length of collided transmission in WLAN (sec)
$T_{pwl}$	364 $\mu$ s	Length of payload in WLAN (sec)
$T_{succwl}$	944 $\mu$ s	Length of successful transmission in WLAN (sec)
$\delta$	1 slot	Duration of Ack wait in ZigBee
$\sigma$	320 $\mu$ s	Length of one backoff unit in ZigBee (sec)
$\sigma_{wl}$	20 $\mu$ s	Unit slot length of one backoff unit in WLAN (sec)

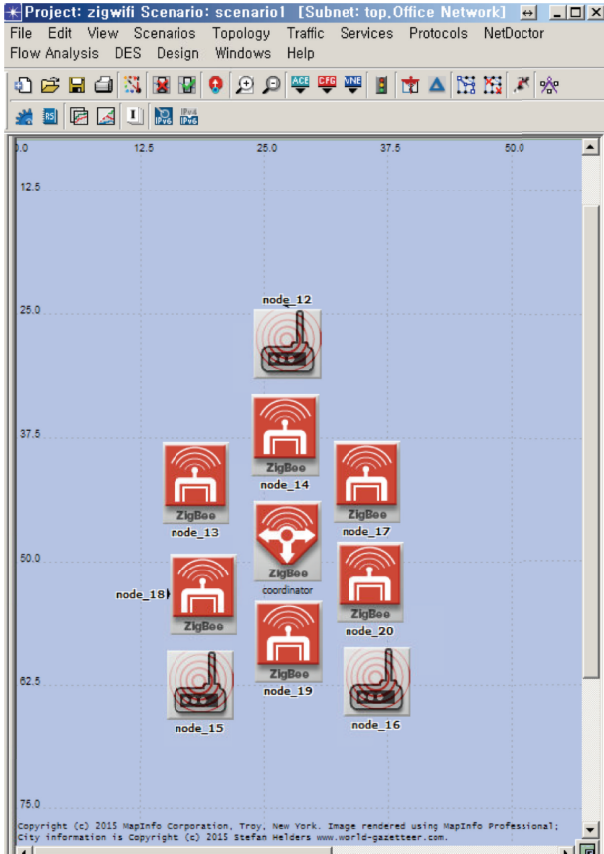


FIGURE 7: Our test coexisting environment.

by the M/G/1 model. Here, the PNC is considered to be equipped with WLAN AP functionality. Figures 14(a) and 14(b) show  $\mathbb{E}\{S\}$  of a ZigBee network, the former without our proposed algorithm and the latter with the algorithm. We initially set the number  $n_{wl}$  of WLAN devices to 0. We sequentially added more WLAN interference load by increasing  $n_{wl}$  to 1, 2, and 3, respectively, and set  $n_{wl}$  back to

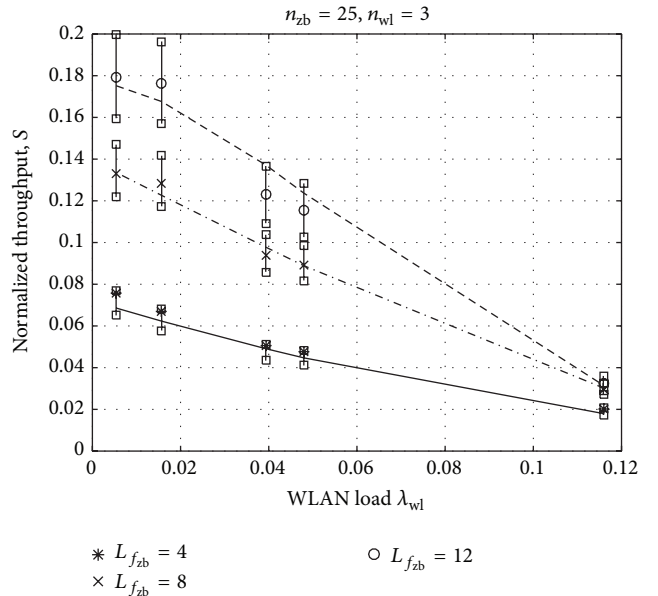


FIGURE 8: Throughput of a ZigBee network interfered with by WLAN devices ( $n_{wl} = 3$ ).

0. Here, the proposed algorithm focuses on controlling the ZigBee frame length  $L_{zb}$  without controlling  $n_{zb}$ , in order to minimize the algorithm computational complexity. The length of ZigBee frames is initially set to 1600 bits. The proposed algorithm shows consequently higher throughput in the overall range of  $n_{wl}$ . For every 5 minutes, the avoidance algorithm shows  $\mathbb{E}\{S\}$  around 170,000, 0, 0, 0, and 170,000 for 0–5, 5–10, 10–15, 15–20, and 20–25 minutes’ intervals, respectively, and the ZigBee operation without the avoidance algorithm gives the same.

For the nonsaturated WLAN mode, the estimation of  $N_{wl}$  needs additional information such as a WLAN traffic model. However, this additional information about the WLAN traffic model is difficult to be known in advance. As mentioned, hence, our model assumes that WLAN devices

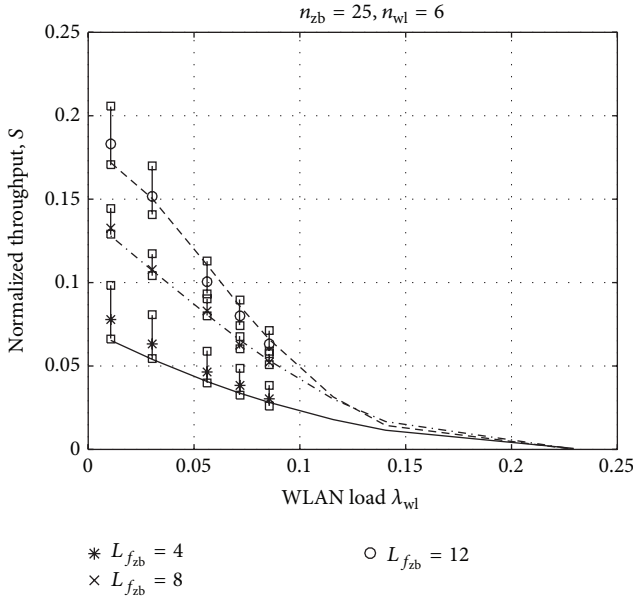


FIGURE 9: Throughput of a ZigBee network interfered with by WLAN devices ( $n_{wl} = 6$ ).

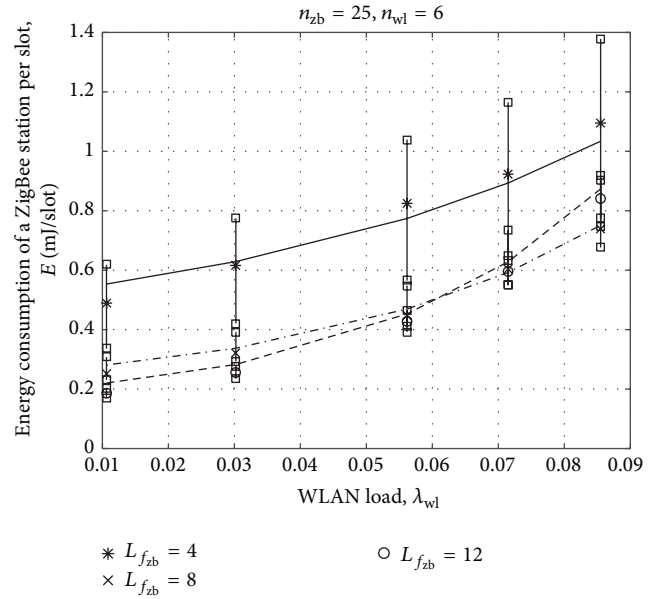


FIGURE 11: Energy consumption of a ZigBee network interfered with by WLAN devices ( $n_{wl} = 6$ ).

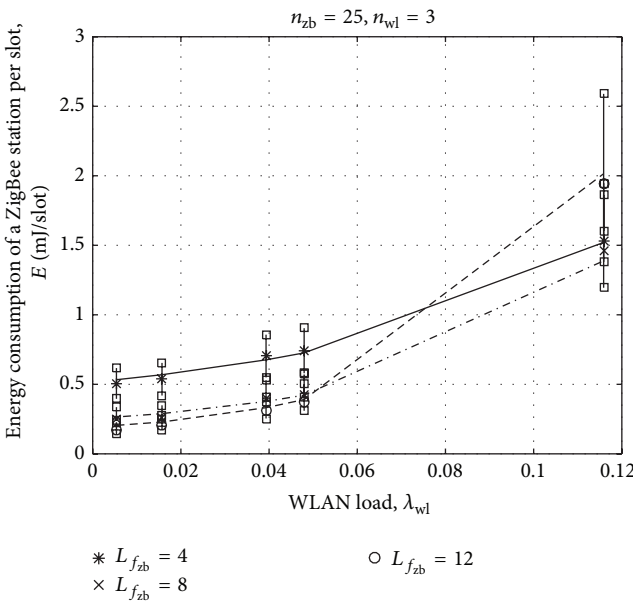


FIGURE 10: Energy consumption of a ZigBee network interfered with by WLAN devices ( $n_{wl} = 3$ ).

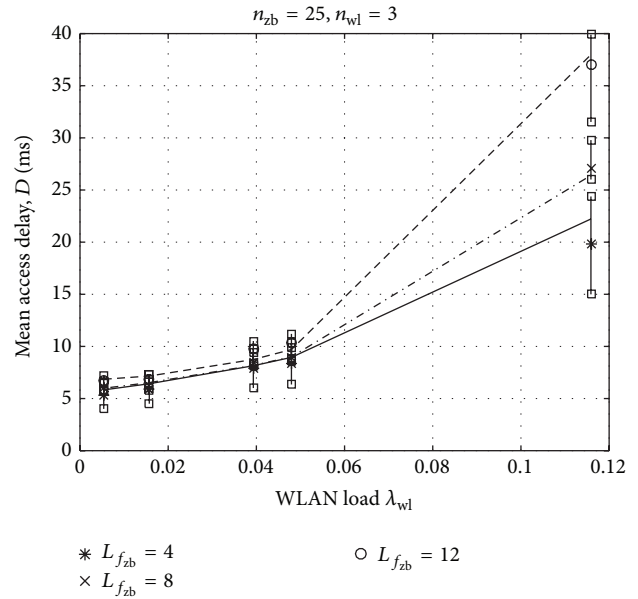


FIGURE 12: Delay of a ZigBee network interfered with by WLAN devices ( $n_{wl} = 3$ ).

highly contend for channel access. The number of interfering WLAN devices is increased by one (from zero to three) every 5 minutes as in the saturated WLAN mode. The length of WLAN frames is set to  $4800 \mu s$  with input load of 0.04 while that of ZigBee frames is initially set to 1600 bits. Here, the proposed algorithm focuses on adapting this length of ZigBee frames  $L_{zb}$  to measured WLAN interference with  $n_{zb}$  maintained. The throughput of the ZigBee network without interference avoidance algorithms is around 170,000, 130,000,

100,000, 70,000, and 170,000 bits/sec for 0–5, 5–10, 10–15, 15–20, and 20–25 minutes’ intervals, respectively, as shown in Figure 15(a). Meanwhile, the proposed avoidance algorithm enhances the performance of the ZigBee network by showing better throughput 170,000, 140,000, 120,000, 105,000, and 170,000 bits/sec for 0–5, 5–10, 10–15, 15–20, and 20–25 minutes’ intervals, respectively, as shown in Figure 15(b). There is no error in measuring  $N_{wl}$  during 5–10 minutes’ interval since  $N_{wl}$  is equal to one. However, errors are introduced in measuring  $N_{wl}$  during 10–15 and 15–20 minutes’ intervals,

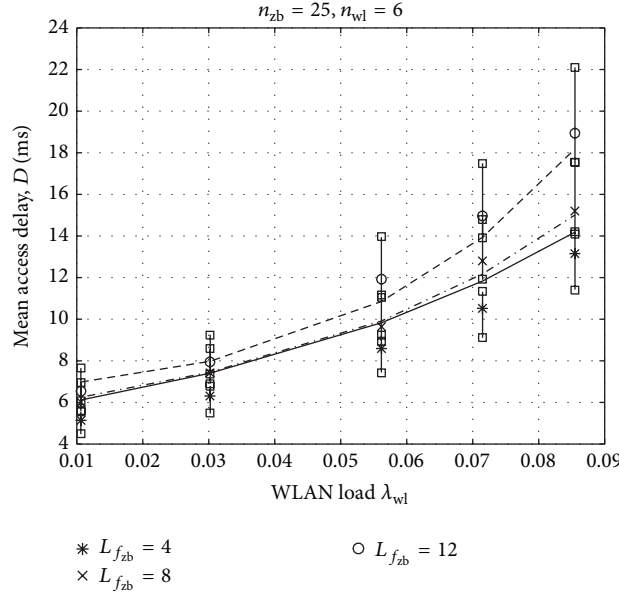


FIGURE 13: Delay of a ZigBee network interfered with by WLAN devices ( $n_{wl} = 6$ ).

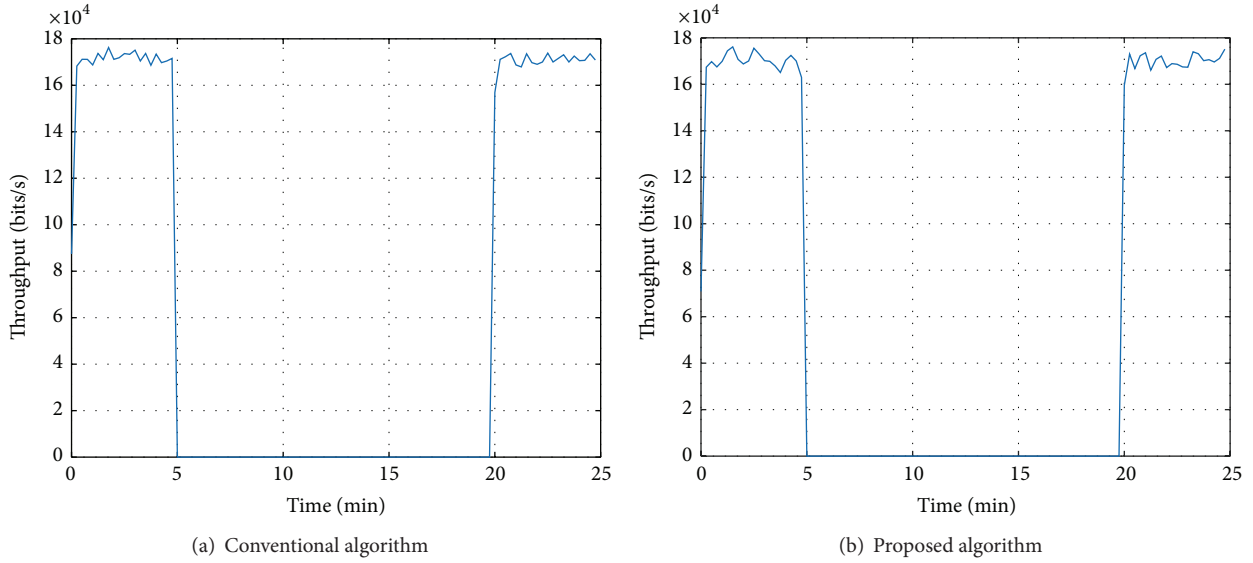


FIGURE 14: Throughput of a ZigBee network with conventional and proposed algorithms interfered with by WLAN in the saturation mode.

that is, three and four, respectively, due to frequent collisions from hidden WLAN nodes. Since the optimum throughput of around 170,000, 145,000, 125,000, 105,000, and 170,000 coming from the accurate estimation of  $N_{wl}$  is higher than the throughput of our proposed algorithm, it gives better results if we can accurately measure  $N_{wl}$ .

### 7. Conclusion

In this paper, we have proposed a unified analysis framework for the ZigBee operation in a ZigBee network interfered with by heterogeneous WLAN networks. Moreover, we proposed an efficient WLAN interference avoidance algorithm for a ZigBee network which controls ZigBee frame length and

devices based on the measured WLAN interference in an adaptive way. WLAN interferences are modeled based on the current IEEE 802.11 to consider realistic effects of interference on a ZigBee network's performance while a ZigBee network is also modeled based on the current IEEE 802.15.4 with a Markov chain concept. The simulation results show a close agreement to the analytical results obtained from our framework. The proposed interference avoidance algorithm has shown the improvement of ZigBee networks' performance by adapting the ZigBee frame length to the WLAN interference level. The simulation results show that the proposed and conventional algorithms give similar performance when the WLAN interferers in the saturated mode interfere with ZigBee networks. However, when the number of WLAN

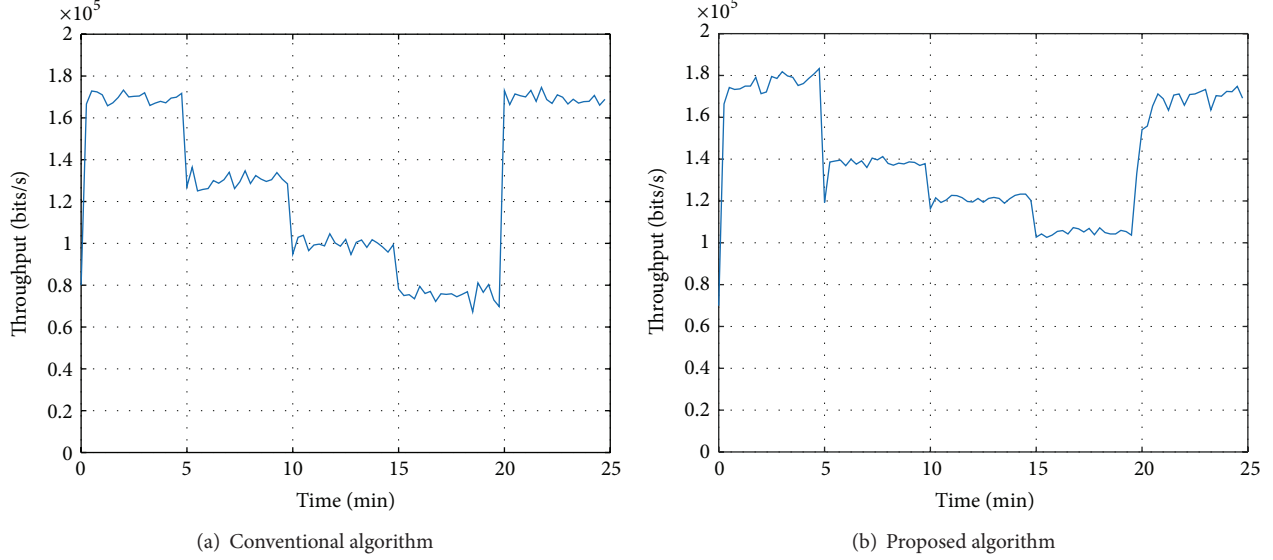


FIGURE 15: Throughput of a ZigBee network with conventional and proposed algorithms interfered with by WLAN in the nonsaturation mode.

interferers is in the nonsaturated mode, the proposed algorithm gives better ZigBee performance than the conventional algorithm. In particular, as the number of nonsaturated WLAN interferers with the input load of 0.04 increases, the proposed algorithm shows a small drop in performance while the conventional algorithm does a large drop. This is due to the algorithm's operation of adapting the length of ZigBee's frames to the measured WLAN interference.

We expect that the proposed analysis framework can be utilized in predicting the performance of ZigBee networks in the presence of heterogeneous WLAN networks as well as design of the parameter settings for efficient ZigBee communication. Also, our proposed unified analysis of a ZigBee network can be applied in predicting and designing various types of coexisting heterogeneous communication networks.

## Appendices

### A. Approximation of $\mathbb{P}\{\Psi_{wl}\sigma_{wl} \leq T_{cca}\}$ , $\mathbb{P}\{\Psi_{wl}\sigma_{wl} > \lceil T_{cca} \rceil + T_{cca}\}$ , and $\mathbb{P}\{\Psi_{wl} = x\}$

$\mathbb{P}\{\Psi_{wl}\sigma_{wl} \leq T_{cca}\}$  can be approximated to  $\mathbb{P}\{\Psi_{wl} \leq \lceil T_{cca}/\sigma_{wl} \rceil\}$ .  $\mathbb{P}\{\Psi_{wl} \leq \lceil T_{cca}/\sigma_{wl} \rceil\}$  means the number of WLAN consecutive idle slots is equal to or smaller than the number of slots, that is,  $\lceil T_{cca}/\sigma_{wl} \rceil$ . This can be derived by the summation of all the probabilities, from the probability that WLAN transmits its frame directly at the first slot to the probability that WLAN transmits at the  $\lceil T_{cca}/\sigma_{wl} \rceil$ th slot as follows:

$$\begin{aligned} \mathbb{P}\{\Psi_{wl}\sigma_{wl} \leq T_{cca}\} &\approx \mathbb{P}\left\{\Psi_{wl} \leq \left\lceil \frac{T_{cca}}{\sigma_{wl}} \right\rceil\right\} \\ &= \left\{1 - (1 - \kappa_{wl})^{n_{wl}}\right\} \sum_{i=0}^{\lceil T_{cca}/\sigma_{wl} \rceil - 1} \left\{(1 - \kappa_{wl})^{n_{wl}}\right\}^i \end{aligned}$$

$$\begin{aligned} &= \left\{1 - (1 - \kappa_{wl})^{n_{wl}}\right\} \frac{\left\{1 - (1 - \kappa_{wl})^{n_{wl}}\right\}^{\lceil T_{cca}/\sigma_{wl} \rceil}}{1 - (1 - \kappa_{wl})^{n_{wl}}} \\ &= 1 - (1 - \kappa_{wl})^{n_{wl} \lceil T_{cca}/\sigma_{wl} \rceil}. \end{aligned} \quad (\text{A.1})$$

Similarly,  $\mathbb{P}\{\Psi_{wl}\sigma_{wl} > \lceil T_{CCA} \rceil + T_{CCA}\}$  and  $\mathbb{P}\{\Psi_{wl} = x\}$  can be expressed as

$$\begin{aligned} &\mathbb{P}\{\Psi_{wl}\sigma_{wl} > \lceil T_{cca} \rceil + T_{cca}\} \\ &\approx (1 - \kappa_{wl})^{n_{wl} \lceil (\lceil T_{cca} \rceil + T_{cca})/\sigma_{wl} \rceil}, \end{aligned} \quad (\text{A.2})$$

$$\mathbb{P}\{\Psi_{wl} = x\} \approx \left\{(\kappa_{wl})^{n_{wl}}\right\}^{x-1} \left\{1 - (1 - \kappa_{wl})^{n_{wl}}\right\}.$$

### B. Approximation of $\rho_{wl+zb}$

We define  $U_{wl}$  as the probability that none of  $n_{wl}$  WLAN devices interfere with ZigBee data transmissions during a ZigBee unit slot, given that the previous slot was not occupied by the transmission of WLAN devices.  $U_{wl}$  can be expressed as  $\{(1 - \kappa_{wl})^{\sigma/\sigma_{wl}}\}^{n_{wl}}$ , where  $\sigma/\sigma_{wl}$  represents the number of WLAN backoff unit slots in a ZigBee unit backoff slot. When the length of a frame is denoted by  $L_{f_x} = \lceil L_f \rceil + \lceil \delta \rceil + \lceil L_{ack} \rceil$ , the average fraction  $\bar{z}$  of the collided part out of  $L_{f_x}$  is expressed as

$$\begin{aligned} \bar{z} &= L_{f_x} - \left\{U_{wl}(1 - U_{wl}) + 2U_{wl}^2(1 - U_{wl}) + \dots \right. \\ &\quad \left. + (L_{f_x} - 1)U_{wl}^{L_{f_x}-1}(1 - U_{wl}) + L_{f_x}U_{wl}^{L_{f_x}}\right\}. \end{aligned} \quad (\text{B.1})$$

Then  $\bar{z}$  is equal to  $L_{f_x} - X$ , where

$$\begin{aligned} X &= U_{wl}(1 - U_{wl}) + 2U_{wl}^2(1 - U_{wl}) + \dots \\ &\quad + (L_{f_x} - 1)U_{wl}^{L_{f_x}-1}(1 - U_{wl}) + L_{f_x}U_{wl}^{L_{f_x}}. \end{aligned} \quad (\text{B.2})$$

Rearranging  $\mathbf{X}$  yields (B.3):

$$(1 - U_{wl})\mathbf{X} = U_{wl}(1 - U_{wl}) + U_{wl}^2(1 - U_{wl}) + \dots + U_{wl}^{L_{fx}-1}(1 - U_{wl}) + U_{wl}^{L_{fx}}(1 - U_{wl}). \quad (\text{B.3})$$

Finally,  $\mathbf{X}$  is derived as

$$\begin{aligned} \mathbf{X} &= U_{wl} + U_{wl}^2 + \dots + U_{wl}^{L_{fx}-1} + U_{wl}^{L_{fx}} \\ &= \frac{U_{wl}(1 - U_{wl}^{L_{fx}})}{(1 - U_{wl})}. \end{aligned} \quad (\text{B.4})$$

Since  $\rho_{wl+zb}$  is defined as the collided ratio due to simultaneous ZigBee and WLAN transmissions,  $\rho_{wl+zb} = \rho_{\bar{z}}/L_{fx}$ .

## Conflict of Interests

The authors declare that there is no conflict of interests regarding the publication of this paper.

## Acknowledgment

This research was supported in part by Basic Science Research Program through the National Research Foundation of Korea (NRF) funded by the Ministry of Science, ICT & Future Planning (NRF-2012R1A1A1041835) and in part by the Research Grant of Kwangwoon University in 2015.

## Endnotes

1. This assumption does not affect the original ZigBee network operation since the tagged ZigBee in the states of  $j > 0$  does not cease to decrease its backoff counter even when the channel is sensed to be busy.
2. If the Markov chain is time-homogeneous, irreducible, positive recurrent, and aperiodic, then the chain converges to the stationary distribution regardless of its initial condition [55]. The stationary distribution  $\pi_{i,j}$  satisfies the equation

$$\boldsymbol{\pi} = \boldsymbol{\pi}\mathbf{P},$$

where  $\boldsymbol{\pi} = [\pi_{i,j}]$  and  $\mathbf{P}$  is state transition probability matrix.

## References

- [1] M. Keshtgari and A. Deljoo, "A wireless sensor network solution for precision agriculture based on zigbee technology," *Wireless Sensor Network*, vol. 4, no. 1, pp. 25–30, 2012.
- [2] C.-J. M. Liang, J. Liu, L. Luo, A. Terzis, and F. Zhao, "RACNet: a high-fidelity data center sensing network," in *Proceedings of the 7th ACM Conference on Embedded Networked Sensor Systems (SenSys '09)*, pp. 15–28, ACM, Berkeley, Calif, USA, November 2009.
- [3] J.-H. Hauer, V. Handziski, and A. Wolisz, "Experimental study of the impact of WLAN interference on IEEE 802.15. 4 body area networks," in *Wireless Sensor Networks*, pp. 17–32, Springer, 2009.
- [4] R. Musaloiu-E and A. Terzis, "Minimising the effect of WiFi interference in 802.15.4 wireless sensor networks," *International Journal of Sensor Networks*, vol. 3, no. 1, pp. 43–54, 2007.
- [5] K. Srinivasan, M. A. Kazandjeva, S. Agarwal, and P. Levis, "The  $\beta$ -factor: measuring wireless link burstiness," in *Proceedings of the 6th ACM Conference on Embedded Networked Sensor Systems*, pp. 29–42, ACM, November 2008.
- [6] C. Won, J. Youn, H. Ali, H. Sharif, and J. Deogun, "Adaptive radio channel allocation for supporting coexistence of 802.15. 4 and 802.11b," in *Proceedings of the IEEE 62nd Vehicular Technology Conference*, vol. 4, pp. 2522–2526, IEEE, 2005.
- [7] M. O. B. Yassien, M. K. Salayma, W. E. Mardini, and Y. M. Khamayseh, "Fibonacci backoff algorithm for IEEE 802.15.4/ZigBee," *Network Protocols and Algorithms*, vol. 4, no. 3, 2012.
- [8] P. Baronti, P. Pillai, V. W. C. Chook, S. Chessa, A. Gotta, and Y. F. Hu, "Wireless sensor networks: a survey on the state of the art and the 802.15.4 and ZigBee standards," *Computer Communications*, vol. 30, no. 7, pp. 1655–1695, 2007.
- [9] J. Zheng and M. J. Lee, *A Comprehensive Performance Study of IEEE 802.15.4*, IEEE Press, Los Alamitos, Calif, USA, 2004.
- [10] G. Lu, B. Krishnamachari, and C. S. Raghavendra, "Performance evaluation of the IEEE 802.15.4 mac for low-rate low-power wireless networks," in *Proceedings of the IEEE International Conference on Performance, Computing, and Communications*, pp. 701–706, 2004.
- [11] C. Buratti, "Performance analysis of IEEE 802.15.4 beacon-enabled mode," *IEEE Transactions on Vehicular Technology*, vol. 59, no. 4, pp. 2031–2045, 2010.
- [12] J. Zheng and M. J. Lee, "Will IEEE 802.15.4 make ubiquitous networking a reality?: a discussion on a potential low power, low bit rate standard," *IEEE Communications Magazine*, vol. 42, no. 6, pp. 140–146, 2004.
- [13] J. A. Gutierrez, M. Naeve, E. Callaway, M. Bourgeois, V. Mitter, and B. Heile, "IEEE 802.15.4: a developing standard for low-power low-cost wireless personal area networks," *IEEE Network*, vol. 15, no. 5, pp. 12–19, 2001.
- [14] S. Pollin, M. Ergen, S. C. Ergen et al., "Performance analysis of slotted carrier sense IEEE 802.15.4 medium access layer," *IEEE Transactions on Wireless Communications*, vol. 7, no. 9, pp. 3359–3371, 2008.
- [15] A. Koubaa, M. Alves, and E. Tovar, "A comprehensive simulation study of slotted CSMA/CA for IEEE 802.15.4 wireless sensor networks," in *Proceedings of the IEEE International Workshop on Factory Communication Systems (WFCS '06)*, pp. 183–192, June 2006.
- [16] I. Ramachandran, A. K. Das, and S. Roy, "Analysis of the contention access period of IEEE 802.15.4 MAC," *ACM Transactions on Sensor Networks*, vol. 3, no. 1, Article ID 1210673, 2007.
- [17] IEEE 802.15.4: Part 15.4: Wireless Medium Access Control (MAC) and Physical Layer (PHY) Specifications for Low-Rate Wireless Personal Area Networks (LR-WPANs), 2003.
- [18] M. Fruth, "Probabilistic model checking of contention resolution in the IEEE 802.15.4 low-rate wireless personal area network protocol," in *Proceedings of the 2nd International Symposium on Leveraging Applications of Formal Methods, Verification and Validation (ISoLA '06)*, pp. 290–297, November 2006.
- [19] V. P. Rao and D. Marandin, "Adaptive backoff exponent algorithm for ZigBee (IEEE 802.15.4)," in *Next Generation Teletraffic and Wired/Wireless Advanced Networking*, vol. 4003

- of *Lecture Notes in Computer Science*, pp. 501–516, Springer, Berlin, Germany, 2006.
- [20] IEEE 802.11: Wireless LAN medium access control (MAC) and physical layer (PHY) specifications, 2007.
- [21] Bluetooth SIG, “Bluetooth specification version 2.0,” 2004.
- [22] S. M. Kim, J. W. Chong, C. Y. Jung et al., “Experiments on interference and coexistence between Zigbee and WLAN devices operating in the 2.4 GHz ISM band,” *Journal of Korean Institute of Next Generation PC*, vol. 1, no. 2, pp. 24–33, 2005.
- [23] K. Shuaib, M. Boulmal, F. Sallabi, and A. Lakas, “Co-existence of ZigBee and WLAN, a performance study,” in *Proceedings of the International Conference on Wireless and Optical Communications Networks (WOCN '06)*, Bangalore, India, 2006.
- [24] A. Sikora and V. F. Groza, “Coexistence of IEEE 802.15.4 with other systems in the 2.4 GHz ISM band,” in *Proceedings of the IEEE Instrumentation and Measurement Technology Conference (IMTC '05)*, vol. 3, pp. 1786–1791, Ottawa, Canada, May 2005.
- [25] N. Golmie, D. Cypher, and O. Rejala, “Performance analysis of low rate wireless technologies for medical applications,” *Computer Communications*, vol. 28, no. 10, pp. 1266–1275, 2005.
- [26] I. Howitt and J. A. Gutierrez, “IEEE 802.15.4 low rate—wireless personal area network coexistence issues,” in *Proceedings of the IEEE Wireless Communications and Networking (WCNC '03)*, vol. 3, pp. 1481–1486, IEEE, New Orleans, La, USA, March 2003.
- [27] D. G. Yoon, S. Y. Shin, W. H. Kwon, and H. S. Park, “Packet error rate analysis of IEEE 802.11b under IEEE 802.15.4 interference,” in *Proceedings of the IEEE Vehicular Technology Conference (VTC Spring '06)*, pp. 1186–1190, Melbourne, Australia, 2006.
- [28] S. Y. Shin, H. S. Park, S. Choi, and W. H. Kwon, “Packet error rate analysis of ZigBee under WLAN and Bluetooth interferences,” *IEEE Transactions on Wireless Communications*, vol. 6, no. 8, pp. 2825–2830, 2007.
- [29] P. Yi, A. Iwayemi, and C. Zhou, “Developing ZigBee deployment guideline under WiFi interference for smart grid applications,” *IEEE Transactions on Smart Grid*, vol. 2, no. 1, pp. 110–120, 2011.
- [30] IEEE 802.15.2: Coexistence of Wireless Personal Area Networks with Other Wireless Devices Operating in Unlicensed Frequency Bands, 2003.
- [31] J. Mišić, S. Shafi, and V. B. Mišić, “Performance of a beacon enabled IEEE 802.15.4 cluster with downlink and uplink traffic,” *IEEE Transactions on Parallel and Distributed Systems*, vol. 17, no. 4, pp. 361–376, 2006.
- [32] T. R. Park, T. H. Kim, J. Y. Choi, S. Choi, and W. H. Kwon, “Throughput and energy consumption analysis of IEEE 802.15.4 slotted CSMA/CA,” *Electronics Letters*, vol. 41, no. 18, pp. 1017–1019, 2005.
- [33] C. Y. Jung, H. Y. Hwang, D. K. Sung, and G. U. Hwang, “Enhanced Markov chain model and throughput analysis of the slotted CSMA/CA for IEEE 802.15.4 under unsaturated traffic conditions,” *IEEE Transactions on Vehicular Technology*, vol. 58, no. 1, pp. 473–478, 2009.
- [34] G. Bianchi, “Performance analysis of the IEEE 802.11 distributed coordination function,” *IEEE Journal on Selected Areas in Communications*, vol. 18, no. 3, pp. 535–547, 2000.
- [35] G. Bianchi and I. Tinnirello, “Remarks on IEEE 802.11 DCF performance analysis,” *IEEE Communications Letters*, vol. 9, no. 8, pp. 765–767, 2005.
- [36] H. Wu, Y. Peng, K. Long, S. Cheng, and J. Ma, “Performance of reliable transport protocol over IEEE 802.11 wireless LAN: analysis and enhancement,” in *Proceedings of the IEEE INFOCOM*, vol. 2, pp. 599–607, San Francisco, Calif, USA, June 2002.
- [37] P. Chatzimisios, A. C. Boucouvalas, and V. Vitsas, “IEEE 802.11 packet delay—a finite retry limit analysis,” in *Proceedings of the IEEE Global Telecommunications Conference (GLOBECOM '03)*, pp. 950–954, San Francisco, Calif, USA, December 2003.
- [38] H. Y. Hwang, S. J. Kim, D. K. Sung, and N.-O. Song, “Performance analysis of IEEE 802.11e EDCA with a virtual collision handler,” *IEEE Transactions on Vehicular Technology*, vol. 57, no. 2, pp. 1293–1297, 2008.
- [39] H. Zhai, Y. Kwon, and Y. Fang, “Performance analysis of IEEE 802.11 MAC protocols in wireless LANs,” *Wireless Communications and Mobile Computing*, vol. 4, no. 8, pp. 917–931, 2004.
- [40] Q. Li and M. Van Der Schaar, “Providing adaptive qos to layered video over wireless local area networks through real-time retry limit adaptation,” *IEEE Transactions on Multimedia*, vol. 6, no. 2, pp. 278–290, 2004.
- [41] K. Duffy, D. Malone, and D. J. Leith, “Modeling the 802.11 distributed coordination function in non-saturated conditions,” *IEEE Communications Letters*, vol. 9, no. 8, pp. 715–717, 2005.
- [42] M. S. Kang, J. W. Chong, H. Hyun, S. M. Kim, B. H. Jung, and D. K. Sung, “Adaptive interference-aware multi-channel clustering algorithm in a ZigBee network in the presence of WLAN interference,” in *Proceedings of the 2nd International Symposium on Wireless Pervasive Computing (ISWPC '07)*, pp. 200–205, IEEE, February 2007.
- [43] D. N. Ko, J. W. Chong, B. H. Jung, and D. K. Sung, “Dynamic clustering schemes of ZigBee networks in the presence of WLAN interference,” in *Proceedings of the Military Communications Conference*, pp. 16–19, San Diego, Calif, USA, November 2008.
- [44] G. Zhou, Y. Wu, T. Yan et al., “A multifrequency MAC specially designed for wireless sensor network applications,” *Transactions on Embedded Computing Systems*, vol. 9, no. 4, article 39, 2010.
- [45] S. Sendra, M. G. Pineda, C. T. Ribalta, and J. Lloret, “WLAN IEEE 802.11 a/b/g/n indoor coverage and interference performance study,” *International Journal on Advances in Networks and Services*, vol. 4, no. 1, pp. 209–222, 2011.
- [46] S. Sendra, J. Lloret, C. Turró, and J. Aguiar, “IEEE 802.11a/b/g/n short-scale indoor wireless sensor placement,” *International Journal of Ad Hoc and Ubiquitous Computing*, vol. 15, no. 1–3, p. 68, 2014.
- [47] M. Fereydooni, M. Sabaei, and G. B. Eslamlu, “Energy efficient topology control in wireless sensor networks with considering interference and traffic load,” *Adhoc & Sensor Wireless Networks*, vol. 25, 2015.
- [48] B. H. Jung, J. W. Chong, S. H. Jeong et al., “Ubiquitous wearable computer (UWC)-aided coexistence algorithm in an overlaid network environment of wlan and ZigBee networks,” in *Proceedings of the 2nd IEEE International Symposium on Wireless Pervasive Computing (ISWPC '07)*, 2007.
- [49] B. H. Jung, J. W. Chong, C. Y. Jung, S. M. Kim, and D. K. Sung, “Interference mediation for coexistence of WLAN and ZigBee networks,” in *Proceedings of the IEEE 19th International Symposium on Personal, Indoor and Mobile Radio Communications (PIMRC '08)*, pp. 1–5, IEEE, September 2008.
- [50] J. Huang, G. Xing, G. Zhou, and R. Zhou, “Beyond co-existence: exploiting WiFi white space for Zigbee performance assurance,” in *Proceedings of the 18th IEEE International Conference on Network Protocols (ICNP '10)*, pp. 305–314, IEEE, Kyoto, Japan, October 2010.
- [51] Y. Wu, G. Zhou, and J. A. Stankovic, “ACR: active collision recovery in dense wireless sensor networks,” in *Proceedings of*

*the 30th IEEE International Conference on Computer Communications (INFOCOM '10)*, pp. 1–9, IEEE, San Diego, Calif, USA, March 2010.

- [52] IEEE 802.11b: Wireless LAN medium access control (MAC) and physical layer (PHY) specifications: Higher-speed physical layer extension in the 2.4 GHz band, 2000.
- [53] IEEE 802.11g, Wireless LAN medium access control (MAC) and physical layer (PHY) specifications: amendment 4: further higher data rate extension in the 2.4 GHz band, 2006.
- [54] J. W. Chong, H. Y. Hwang, C. Y. Jung, and D. K. Sung, “Analysis of throughput in a ZigBee network under the presence of WLAN interference,” in *Proceedings of the International Symposium on Communications and Information Technologies (ISCIT '07)*, pp. 1166–1170, IEEE, Sydney, Australia, October 2007.
- [55] W. R. Gilks, S. Richardson, and D. J. Spiegelhalter, *Markov Chain Monte Carlo in Practice*, Chapman & Hall, London, UK, 1996.
- [56] J. R. Norris, *Markov Chains*, Cambridge University Press, Cambridge, UK, 1997.
- [57] G. Bianchi and I. Tinnirello, “Kalman filter estimation of the number of competing terminals in an IEEE 802.11 network,” in *Proceedings of the 22nd Annual Joint Conference of the IEEE Computer and Communications Societies (INFOCOM '03)*, vol. 2, pp. 844–852, IEEE, San Francisco, Calif, USA, April 2003.





**Hindawi**

Submit your manuscripts at  
<http://www.hindawi.com>

